



## The upper limit of maturity of natural gas generation and its implication for the Yacheng formation in the Qiongdongnan Basin, China

Long Su<sup>a,b,\*</sup>, Jianjing Zheng<sup>a</sup>, Guojun Chen<sup>a</sup>, Gongcheng Zhang<sup>c</sup>, Jianming Guo<sup>a</sup>, Yongchang Xu<sup>a</sup>

<sup>a</sup> Key Laboratory of Petroleum Resources Research, Institute of Geology and Geophysics, Chinese Academy of Sciences, Lanzhou, Gansu 730000, PR China

<sup>b</sup> Graduate University of the Chinese Academy of Sciences, Beijing 100039, PR China

<sup>c</sup> Research Institute of China National Offshore Oil Corporation, Beijing 100027, PR China

### ARTICLE INFO

#### Article history:

Received 27 July 2011

Received in revised form 30 November 2011

Accepted 17 April 2012

Available online 27 April 2012

#### Keywords:

Hydrocarbon source rock

Yacheng Formation

Pyrolysis experiment

Upper limit of maturity for natural gas

generation

Qiongdongnan Basin

### ABSTRACT

Vitrinite reflectance (VR, Ro%) measurements from residual kerogen of pyrolysis experiments were performed on immature Maoming Oil Shale substituted the samples for the gas-prone source rocks of Yacheng formation of the Qiongdongnan Basin in the South China Sea. The work was focused on determination an upper limit of maturity for gas generation (ULMGG) or “the deadline of natural gas generation”. Ro values at given temperatures increase with increasing temperature and prolonged heating time, but  $\Delta Ro$ -value, given a definition of the difference of all values for VR related to higher temperature and adjacent lower temperature in open-system non-isothermal experiment at the heating rate of 20 °C/min, is better than VR. And representative examples are presented in this paper. It indicates that the range of natural gas generation for Ro in the main gas generation period is from 0.96% to 2.74%, in which  $\Delta Ro$  is in concordance with the stage for the onset and end of the main gas generation period corresponding to 0.02% up to 0.30% and from 0.30% up to 0.80%, respectively. After the main gas generation period of 0.96–2.74%, the evolution of VR approach to the ULMGG of the whole rock for type II kerogen. It is equal to 4.38% of VR, where the gas generation rates change little with the increase of maturation,  $\Delta Ro$  is the maximum of 0.83% corresponding to VR of 4.38%Ro, and the source rock does not nearly occur in the end process of hydrocarbon gas generation while Ro is over 4.38%. It shows that it is the same the ULMGG from the whole rock for type II kerogen as the method with both comparison and kinetics. By comparing to both the conclusions of pyrolysis experiments and the data of VR from the source rock of Yacheng formation on a series of selected eight wells in the shallow-water continental shelf area, it indicate that the most hydrocarbon source rock is still far from reaching ULMGG from the whole rock for type II kerogen. The source rock of Yacheng formation in the local areas of the deepwater continental slope basin have still preferable natural gas generative potential, especially in the local along the central depression belt (namely the Ledong, Lingshui, Songnan and Baodao sags from southwest to northeast) from the depocenter to both the margin and its adjacent areas. It help to evaluate the resource potential for oil and gas of the hydrocarbon source rock in the deepwater continental slope of the Qiongdongnan Basin or other basins with lower exploration in the northern of the South China Sea and to reduce the risk in exploration.

© 2012 Elsevier Ltd. All rights reserved.

### 1. Introduction

There are many maturation parameters available, such as VR, spore coloration,  $T_{max}$  from Rock-Eval pyrolysis, Apatite Fission Track Analysis, but VR is the most commonly used (Carr and Williamson, 1990; Huang, 1996). Traditionally, the current wisdom is to consider VR as a function of temperature and time (Hunt, 1979; Tissot and Welte, 1984). And some observations confirm

that the development of VR is controlled more by temperature than time, especially the importance of temperature as opposed to time in controlling maturation has been presented (Ritter, 1984; Huang, 1996), which is consistent with kinetically based models of VR in which reflectance is exponentially related to temperature, but only linearly related to time. Furthermore, many maturity models which explorationists have developed are either Lopatin's Time–Temperature Indexes (TTIs) produced by calibrating the maturity with time and temperature in basins (Waples, 1980; Goff, 1983), or kinetically based (Ritter, 1984; Sweeney and Burnham, 1990; Li et al., 2008). Recently, more laboratory studies focus on the effects of pressure on VR (Price and Wenger, 1992; Hao et al., 1995) which have shown that pressure or over-

\* Corresponding author at: Key Laboratory of Petroleum Resources Research, Institute of Geology and Geophysics, Chinese Academy of Sciences, Lanzhou, Gansu 730000, PR China. Tel.: +86 931 4960850.

E-mail address: [sulong08@163.com](mailto:sulong08@163.com) (L. Su).

pressure can be incorporated into a kinetic model (Dalla Torre et al., 1997; Carr, 1999, 2000; Zou and Peng, 2001), and on any other parameters capable of influencing the maturity, e.g. heating rate, lithology, hydrogen index and dry or wet conditions in laboratory pyrolysis (Khorasani and Michelsen, 1994; Huang, 1996; Lewan, 1998). Generally, these methods for modeling the behavior of organic matter at depth in the source kitchens, in that exploration drilling rarely encounters the source kitchens responsible for hydrocarbon generation.

The hydrocarbon source rock of Yacheng formation (early Oligocene) in the Qiongdongnan Basin (QDNB) of the South China Sea (SCS) is buried deeply at the high subsidence rate during Oligocene–Quaternary (Sun, 1994; Gong et al., 1997; Yuan et al., 2008) and matured rapidly, and had been at high-maturity or over-mature stage (Huang, 1999). According to the classic theory and modeling on the hydrocarbon generation by kerogen thermo-decomposition by Tissot and Welte (1984), it can be assumed that a large quantity of liquid hydrocarbons and natural gases had been generated during the mature stage from the organic matter of these source rocks. The questions remaining are how much

the gas generative potential is during Oligocene–Quaternary, and how much the gas generative potential is at the high-maturity or over-mature stage, and whether or not they could form commercial natural gas pools. To answer these questions will not only help to resolve many problems in mechanism of hydrocarbon accumulation of the SCS, but also determine whether the layer system and blocks of the exploration in deepwater areas of the QDNB select or not. And it is one of the key issues whether or not enhance to launch the large-scale exploration in the deepwater region of the QDNB.

So, as a maturation parameters available of VR (Ro), the work was focused on determination a ULMGG or the deadline of gas generation by pyrolysis experiments under various conditions for the hydrocarbon source rock of Yacheng formation in the QDNB. To obtain the geological conditions of a sedimentary basin, we analyze the geologic, thermal and buried history of the hydrocarbon source rock and the geological features in deepwater area of the QDNB on the comprehensive research of the previous. It can be checked by comparing different pyrolysis experiments of one sample, in order to accelerate the prospecting of oil and gas in the deepwater basin

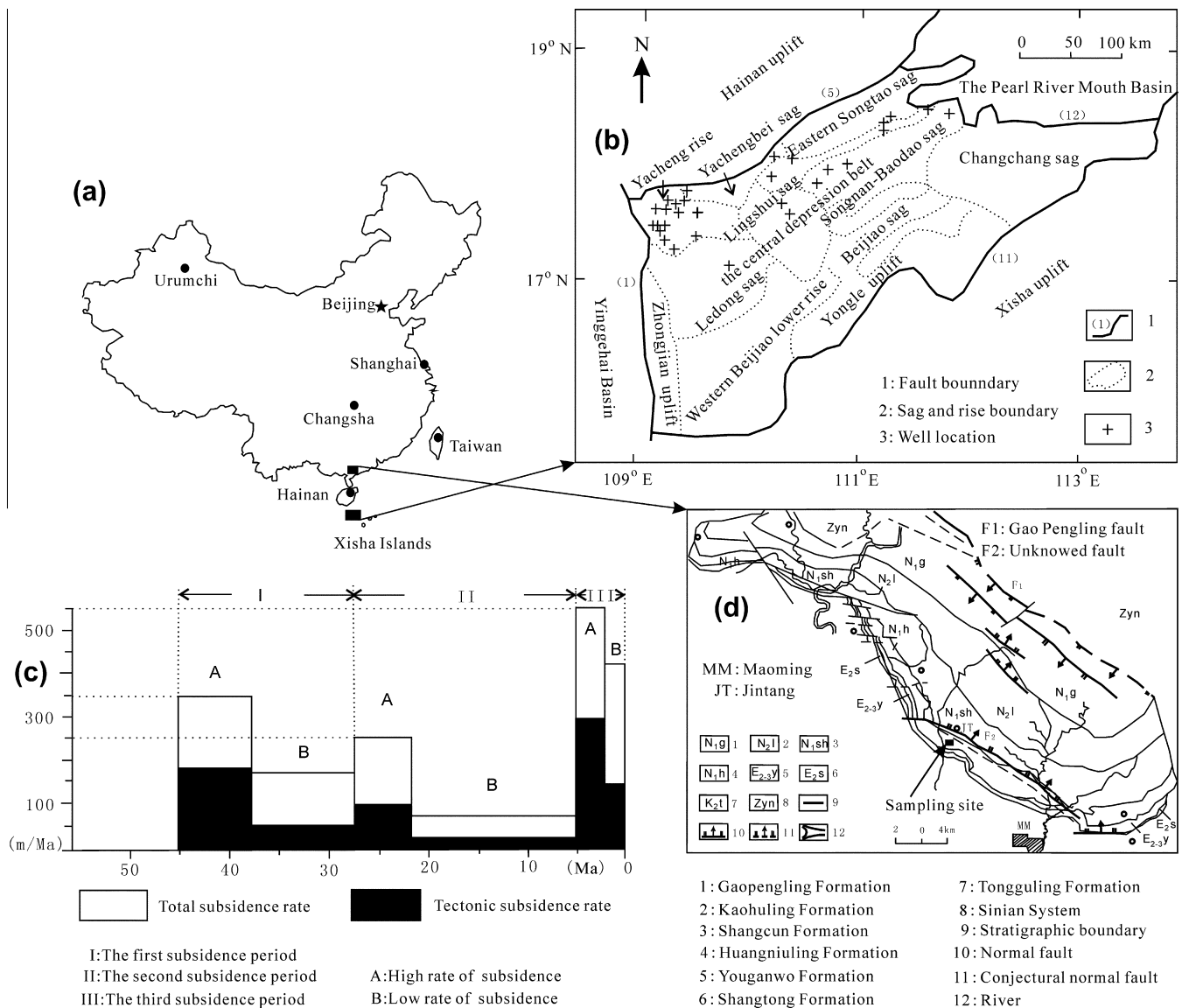


**Fig. 1.** Map showing: (a) the locations of the Qiongdongnan in the South China Sea and Maoming basin; (b) tectonic units, locations of the wells and the No. 1 fault, No. 5 fault, No. 11 fault and No. 12 fault in the Qiongdongnan Basin; (c) total and tectonic subsidence rate of selected seismic profile in the Qiongdongnan Basin; (d) the geological map of Maoming basin and sampling site. (b) Is revised after Yuan et al., 2008 and Zhang et al., 2010, (c) Is revised after Gong et al., 1997 and (d) Is cited after Guo et al., 2009).

of the SCS. It will help to forecast preferable prospect area and to establish exploration strategy. Especially some large-scale oil and gas fields in the deepwater continental slope of the petroliferous basins around the world were found one after the other.

## 2. Geologic setting

The QDNB is one of the oil–gas bearing basins in the northern continental margin of the SCS. The basin is lying between Hainan Island and the Xisha Islands (Fig. 1a and b), covering an area of about 30,000 km<sup>2</sup>. The geology of the QDNB has been reported (Yu et al., 1999; Yuan et al., 2008; Zhu et al., 2008; Zhang et al., 2010). Briefly, it is separated from Hainan uplift by the No. 5 fault in the north (Fig. 1b), Xisha–Zhongsha uplift by the No. 11 fault in the south, Yinggehai Basin by the No. 1 fault in the west and Pearl River Mouth Basin by the No. 12 fault in the east (Li and Zhu, 2005). Its western part is a deep depression containing Cenozoic strata more than 10 km thick, especially the maximum of burial depth with prominent local sag in the central depression belt is about 12 km, according to drilling data and seismic data (Zhu et al., 2008; Zhang et al., 2010). The central depression belt include the Ledong, Lingshui, Songnan, and the Baodao sags from southwest to northeast. The basement of the basin is dominated by the granite forming in Yanshan period with a few Paleozoic sedimentary and metamorphic rocks, which is buried at depth 9–13 km in the Ledong sag, 8–12 km in the Lingshui sag, 7–10 km in the Songnan sag and 7–11 km in the Baodao sag (Yu et al., 1999). Its sedimentary sequences, from bottom to top, are Eocene, Yacheng formation (early Oligocene), Lingshui formation (late Oligocene), Sanya formation (early Miocene), Meishan formation (middle Miocene), Huangliu formation (late Miocene), Yinggehai formation (Pliocene), and Ledong formation (Quaternary), respectively. It experienced multi-episodic extensional rifting, and therefore multi-episodic heating events in Cenozoic time (He et al., 2001; Yuan et al., 2009). The initial, early, and late rifting phases corresponded to the Paleocene, Eocene, and Oligocene heating events, respectively.

The current geothermal field in the QDNB have been discussed in a series of studies (He et al., 2001; Shi et al., 2003; Yuan et al., 2009; Mi et al., 2009; Zhang et al., 2010). It synthesized the recent advances in researches is associated with “hot basin” by high-maturity, high heat flow and high geothermal gradient with respect to the basin developed in the South China continent. The distribution of the present geotemperature at the bottom of Yacheng formation reported is about 100–400 °C (Zhang et al., 2010). The heat flow of the basin reaches the value of  $72.9 \pm 14.2$  mW/m<sup>2</sup>, about 79 mW/m<sup>2</sup> in the central depression estimated (Shi et al., 2003) and its geothermal gradient varies from 19.7 °C/km and 39.5 °C/km with an average of  $31.9 \pm 5.6$  °C/km (Yuan et al., 2009). The heat flow and geothermal gradient of the basin tend to increase from the continental shelf to continental slope (Shi et al., 2003; Yuan et al., 2009). It is the combination of the Cenozoic lithospheric thinning (He et al., 2001; Shi et al., 2003) and the magnitude of the lithospheric thinning through adjustment of the stress field at depth in the SCS (Zhan et al., 2006). Moreover, it was controlled by the magmatic activities and faulting during the Neotectonic event that the present-day geothermal field in the QDNB (Mi et al., 2009). The Neotectonic period occurred in the Pliocene (Yu et al., 1999; Zhang et al., 2007), which accounts for the rapid subsiding in the QDNB since 10.5–5.3 Ma (Yuan et al., 2008). And the final episode of rapid subsiding event started earlier in the west than that in the east. The Ledong sag of western QDNB started the third rapid subsiding at ~10.5 Ma, while the central and eastern QDNB did not begin to sink until 5.3 Ma.

Since the Neotectonic period, QDNB is characterized with a large subsidence, the deposition at high-speed rate and a wide

sedimentary range, together. Its total subsidence rate is over 200 m/Ma (Sun, 1994) in the central depression belt and up to 550 m/Ma, such as seismic profile (Gong et al., 1997) in the QDNB (Fig. 1c). The maximum of the tectonic subsidence rate was as high as 257 m/Ma in the Ledong sag of western QDNB, decreased to 179 m/Ma in the Lingshui sag of central QDNB and was as low as 29 m/Ma in eastern QDNB (Yuan et al., 2008). It is prominent that the sag in the western parts of the QDNB in the late period is dominated profoundly by the Neotectonic event. So, the hydrocarbon source rock of Yacheng formation (early Oligocene) in the QDNB was buried deeply at the high subsidence rate and matured rapidly and had been at a high-maturity or over-mature stages (Huang, 1999). The basin is filled with the source rocks of the lacustrine mudstones in Eocene, lacustrine facies, limnetic facies and transitional facies in Oligocene and deposits in Miocene (Zhu et al., 2008; He et al., 2009). The hydrocarbon source rocks of Yacheng formation with kerogen of II<sub>2</sub>–III type is one of the major hydrocarbon source rocks which have great contribution to oil and gas generation (Gong et al., 1997; Zhang et al., 2007; Zhu et al., 2008).

## 3. Experiment

### 3.1. Substituted sample

Because of the lower exploration of oil and gas in the deepwater continental slope area and a high-maturity of the hydrocarbon source rock from petroleum exploration wells in the shallow-water continental shelf region in the QDNB (Zhu et al., 2008; He et al., 2009), we cannot collect the samples reliable for the experiments. And in view of insufficient well logging data and shortage of geological information for the deepwater continental slope area (He et al., 2009), the same work of the ULMGG as statistical rules from the hydrocarbon source rocks of various types of kerogen and different maturation with the presence of considerable amounts of samples cannot do as the previous study (Wang et al., 2005; Chen et al., 2007). But it is one of the urgent problems need to be answered what is the ULMGG from the hydrocarbon source rock to current prospect and exploration for oil and gas in the deepwater continental slope basin of the broad areas in the ocean of China. Therefore, a oil shale sample substituted for Yacheng formation collected from the Maoming basin (Fig. 1d), where the basic geological conditions of the source rock for the same history of sedimentary, parent material, and depositional environment and accumulation in basin are similar to QDNB by comparison to large geological information of the SCS and adjacent areas in China. On the other hand, the experiments are conducted by the direct use for the immaturity hydrocarbon source rock of whole rock according to the compositions of the inorganic substances under the geological conditions and requirements of measuring accuracy for the thermal simulation products (Geng et al., 2005). The genesis and structure of Maoming Oil Shale have been extensively studied in the last two decades (Fu et al., 1985; Hou et al., 1989; Yu et al., 2000; Guo et al., 2009), providing good reference data for our study. The analysis of sedimentary environments of Maoming basin shows that the source rock is formed in semi-deep to deep lacustrine and limnetic environments. Especially, Youganwo formation in Oligocene is one of the major hydrocarbon source rocks in Maoming basin (Guo et al., 2009).

The sample thus used in the present experiments is under depth about 80 m from surface of the upper fault in a famous oil-shale producing mining area in Jintang of Maoming basin. And at this locality it is thermally immature in the pre-oil generation stage. A fresh unweathered sample was collected from a 20 cm thick bed 30 cm below the upper contact with an overlying gray mudstone. The collected sample is a brown rock with an organic carbon

**Table 1**  
Total organic carbon (TOC) and Rock–Eval pyrolysis data on the sample using in closed and open system experiments.

Location of samples	Stratum	TOC (%)	S <sub>1</sub> -peak (mg/g rock)	S <sub>2</sub> -peak (mg/g rock)	Ro (%)	T <sub>max</sub> (°C)
Mining area in Jintang of Maoming basin	Youganwo formation	11.40	1.24	55.36	0.44	431

content of 11.40%, and Ro is 0.44%. And type II kerogen of the Maoming Oil Shale has an atomic H/C ratio of 1.65 and an atomic O/C ratio of 0.19 as Hou et al. (1989). General organic geochemical characteristics of the original rock sample from Rock–Eval pyrolysis are summarized in Table 1. VR and T<sub>max</sub>-value clearly indicate that the organic matter of the rock is immature.

### 3.2. Experimental conditions

#### 3.2.1. Hydrous pyrolysis in the closed-system of autoclave

The hydrous pyrolysis experiment in the closed-system were performed in 200 ml autoclaves of Hastelloy GCF-0.25 L reactor (made in Dalian city, Liaoning province of China). The samples were grounded to 80 mesh. In each experiment about 50 g of the powdered samples material of whole rock and deionized water given 12, 10, 8, 6 and 4 ml at maximum heating temperature were used as advised by Qin et al. (2002), respectively. Before closing, the autoclaves were purged with helium. After the oven temperature was programmed from air temperature about 20 °C to 300 °C (an initial heating) and to the next temperature at 3 °C/min, and then held at this temperature for 72 h. Then the next temperature was increased in steps of 50 °C up to the final temperature for each experiment, maximally to 500 °C. Different duration (72, 144 and 216 h) were used at the final temperature level (500 °C) in order to obtain the rate of hydrocarbon gas generation and evolution of VR under the same temperature against various duration. The autoclaves were air-cooled to ambient temperature overnight before sampling and analyses. Temperatures were monitored with type XMT-131 thermocouples that were calibrated against national standards at the final temperature for each experiment. After the experiments cooled to room temperature, pressure and temperature were recorded and a sample of head-space gas was collected in an evacuated 30 cm<sup>3</sup> stainless-steel cylinder.

#### 3.2.2. Anhydrous pyrolysis in the open-system non-isothermal experiment

The method of anhydrous pyrolysis under open-system conditions provides probably the closest approach to primary cracking reactions. In each experiment the organic material of whole rock was pyrolyzed in the open-system non-isothermal pyrolysis as described by Krooss et al. (1995) on a new apparatus, which has been built in 2009 by the Key Laboratory of Petroleum Resources Research in Institute of Geology and Geophysics of Chinese Academy of Sciences. Fig. 2 shows a scheme of the experimental set-up. The equipment consists of an open system pyrolysis furnace with ultra-high temperature as well as a computerized remote control and data sampling unit. For rock pyrolysis, an open system pyrolysis unit designed for dry non-isothermal experiments was

used and heated from 250 °C (an initial heating) and up to 1100 °C (an final heating), increasing in steps of 50–1100 °C by controlling the oven temperature with Eutrotherm™ during the experiments. It was carried out in sealed quartz glass reactor of the apparatus with low pressures, and very large reaction volumes relative to the large amounts of reactants about 30 g of the powdered samples material.

The reactor was heated in a horizontal single furnace. It was equipped with an internal metal coat to homogenize the temperature field around the rock material. Based on NiCr–Ni thermocouples within the metal coat and directly dipping into the sample, the accuracy of the temperature measurement resulted in an error of about ±2 °C. The quartz glass reactor was then closed and flushed with helium current for 50 min to remove atmospheric gas and permanently flushed with 30 ml/min helium as carrier gas during the pyrolysis. After setting the constant heating rates of 8 or 20 °C/min, maximum temperature and checking the flange leakage, the experiment commenced and ran automatically. And the higher heating rate of 20 °C/min was designed on the basis of the high geothermal field in the QDNB. For compositions of gas phase products analyses, gas samples were taken off-line from experiments performed. During time intervals (approximately 6 and 2.5 min corresponding to heating rate of 8 and 20 °C/min) gaseous pyrolysis products together with helium were flushed through an annulations equipped with two stopcocks linked to a group of glass sampling flask (250 ml). After regular intervals gas was expanded into a glass sampling flask and it was closed for No. 1 at 250 °C and to No. 18 at 1100 °C. For every gas samples a new glass flask was installed.

For compositions of hydrocarbon gas analyses, and the gas sample of carrier gas was injected from the glass flask into a gas chromatography (HP 6890) unit and gaseous hydrocarbons were separated and quantified system analysis by gas chromatographic analysis. The rates of generation for methane, ethane, propane and heavy hydrocarbons (C<sub>4–6</sub>) using the respective peak areas and the known concentration of the components in the calibration standard above. Measurements were carried out using the method of continuous flow. Due to the reproducibility of the experiment, a repeat run at 20 °C/min was performed for about 30 g of the powdered samples not only measuring compositions of hydrocarbon gas but also obtaining VR of residual kerogen from the pyrolysis experiment at every given temperature. During the experimental procedure, all glass apparatus, flask and vials were thoroughly cleaned and baked at 550 °C for 4 h before using in order to avoid any possible laboratory contamination.

Additionally, VR of original sample and pyrolysis residues from the anhydrous and hydrous experiments were measured using microscope photometer of type UMSP-50 in accordance with the

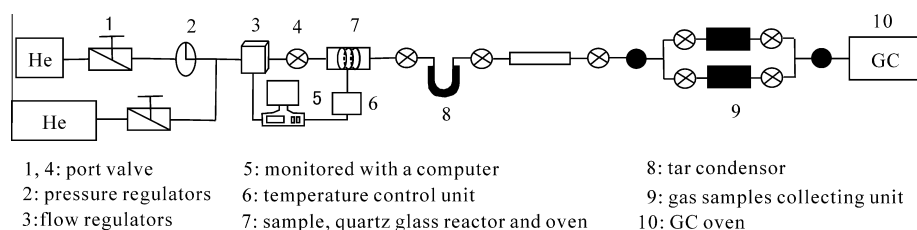


**Fig. 2.** Scheme of the experimental system used in the open-system non-isothermal experiment.

State Standard of China SY/T 5124-1995 (equivalent to ISO 7404-5:1994). The evaluation of the experimental data was performed according to the scheme and yielded an activation energy distribution and one common pre-exponential factor for the entire set of parallel reactions with the special kinetics software (edition in 2005) as the model of LLNL (Lawrence Livermore National Laboratory) in USA.

## 4. Results and discussion

### 4.1. Kinetic parameters of hydrocarbon gas generation

The method used in this kinetic study was open-system non-isothermal pyrolysis as Krooss et al. (1993). The temperature of the generation yields for methane obtained is range from 250 to 1100 °C. In order to obtain the ULMGG, the temperature is available up to 1100 °C in the present. Kerogen pyrolyzed thoroughly under this ultra-high temperature and gaseous pyrolysis products are expelled from the reactors by helium as carrier gas while they are generating from the pyrolyzed rocks and could be recorded completely. The hydrocarbon gas generation maximum was therefore sufficiently defined with respect to its peak shape and the overall generation potential. Based on the experimental generation yields activation energy distributions for the generation of methane, ethane, propane and heavy hydrocarbon components (C<sub>4-6</sub>) from the samples were determined.

The kinetic evaluation of the experimental data is under the simplifying assumptions that: (i) the generation reactions of both gases could be explained by a set of parallel first-order reactions with Arrhenius-type temperature dependence, (ii) the pre-exponential factor for all reactions are identical, and (iii) the sequence of reactions in the laboratory is the same as in nature, where much more time is available and where temperatures are much lower. The precision of the kinetic parameters, in particular the pre-exponential factor, can be improved by performing pyrolysis experiments at different heating rates of 8 and 20 °C/min, which the latter is high on the basis of the present-day high geothermal fields in the QDNB.

Krooss et al. (1993) have been reported activation energy distributions for the generation of nitrogen and methane but not related to that ethane, propane and heavy hydrocarbons (C<sub>4-6</sub>) as intermediate pyrolysis products. In this study, we calculated activation energy for the generation of not only methane but also ethane, propane and heavy hydrocarbons (C<sub>4-6</sub>) from oil shale sample. For the kinetic evaluation of the experimental data it is assumed that the generation of hydrocarbon gas from organic matter can be described by a set of parallel reactions following a first-order rate law (Braun and Burnham, 1987). The reaction rate,  $r_i$ , of the  $i$ th parallel reaction is expressed as:

$$r_i = dm_i/dt = k_i(m_{0i} - m_i) \quad (1)$$

where  $m_{0i}$  is the total amount of gas that can be generated from the oil shale (ultimate gas yield) via reaction  $i$  and  $m_i$  is the amount of gas that has been generated by this reaction until time  $t$ . The temperature dependence of the rate coefficients ( $k$ ) of kerogen maturation (Sweeney and Burnham, 1990) and petroleum generation

reactions is commonly expressed by the semi-empirical Arrhenius equation which represents a good approximation of relationships derived on a more rigorous theoretical basis:

$$k_i = A_i \exp(-E_i/RT) \quad (2)$$

where  $A_i$  is pre-exponential factor of the  $i$ th reaction ('frequency factor') ( $s^{-1}$ ),  $E_i$  is activation energy of the  $i$ th reaction (J/mol),  $T$  is absolute temperature (K),  $R$  is the gas constant (J/mol/K). Evaluations were carried out assuming up to 25 parallel reactions ( $i = 1-25$ ) each of which was attributed a specific activation energy.

In order to reduce the number of parameters the same pre-exponential factor  $A$  was taken for all reactions ( $A_i = A$  for all  $i$ ). The sample was pyrolyzed at two different heating rates in order to achieve a more reliable determination of the kinetic parameters, in particular the pre-exponential factor. Using a non-linear least-squares fit procedure (Schaefer et al., 1990) the generation potentials ( $m_{0i}$ ) for the  $i$  reactions and the common pre-exponential factors were adjusted to obtain the best fit of the calculated generation yields to the experimental curves for two heating rates with the special kinetics software. The results of the kinetic evaluation for hydrocarbon gas generation from the oil shale in terms of an activation energy distribution are shown in Table 2 and Fig. 3. The activation energies and corresponding pre-exponential factors for methane, ethane, propane, and heavy hydrocarbons (C<sub>4-6</sub>) obtained from this evaluation are in the range from 38 to 86 kcal/mol at  $6.47 \times 10^{11}$  (1/s), 44 to 92 kcal/mol at  $2.70 \times 10^{12}$  (1/s), 43 to 77 kcal/mol at  $1.10 \times 10^{15}$  (1/s) and 46 to 70 kcal/mol at  $8.39 \times 10^{15}$  (1/s), respectively. These pre-exponential factors are similar with values of around  $10^{11}$ – $10^{12}$  (1/s) to those reported by Pepper and Corvi (1995) and slightly higher values of  $10^{13}$ – $10^{15}$  (1/s) (Espitalié et al., 1988; Forbes et al., 1991; Braun and Burnham, 1992; Béhar et al., 1997).

Activation energy distributions of hydrocarbon gas generation show an asymmetrical appearance. In order of methane, ethane and propane of all evaluations performed, the dominant frequency of activation energy and its percent for those hydrocarbon gases increasing gradually are from 52 to 63 kcal/mol and from 20.44% to 42.50%, respectively. And corresponding pre-exponential factors increased exponentially from  $6.47 \times 10^{11}$  to  $1.10 \times 10^{15}$ . Furthermore, comparison to methane, ethane and propane both the decrease of activation energy and the exponential increase of pre-exponential factor for heavy hydrocarbons will have a greater contribution to the constant of the reaction rate ( $R$ ) according to Eq. (2). Further measurements to verify these kinetic parameters are in progress.

### 4.2. Expression and determination of the main generation period for natural gas

It is difference between the hydrocarbon generation and the evolution for various types kerogen. Even if the same type of kerogen, the previous studies have shown that it is different between the hydrocarbon generation process and gas generation rates in various stages by using different simulation systems (Hu et al., 2004; Zhao et al., 2005). Therefore, the main gas generation period under different experimental systems must be obtained first accu-

**Table 2**  
Kinetic parameters of hydrocarbon gas generation results for type II organic matters.

Parameters	C <sub>1</sub>	C <sub>2</sub>	C <sub>3</sub>	C <sub>4-6</sub>
Distribution of activation energy (kcal/mol)	38–86	44–92	43–77	46–70
Dominant frequency of activation energy (kcal/mol)	52	54	63	48
Percent of dominant frequency of activation energy (%)	20.44	38.04	42.5	25.05
Pre-exponential factor ( $s^{-1}$ )	$6.47 \times 10^{11}$	$2.70 \times 10^{12}$	$1.10 \times 10^{15}$	$8.40 \times 10^{15}$

C<sub>1</sub>: Methane; C<sub>2</sub>: Ethane; C<sub>3</sub>: Propane; C<sub>4-6</sub>: Heavy hydrocarbons.

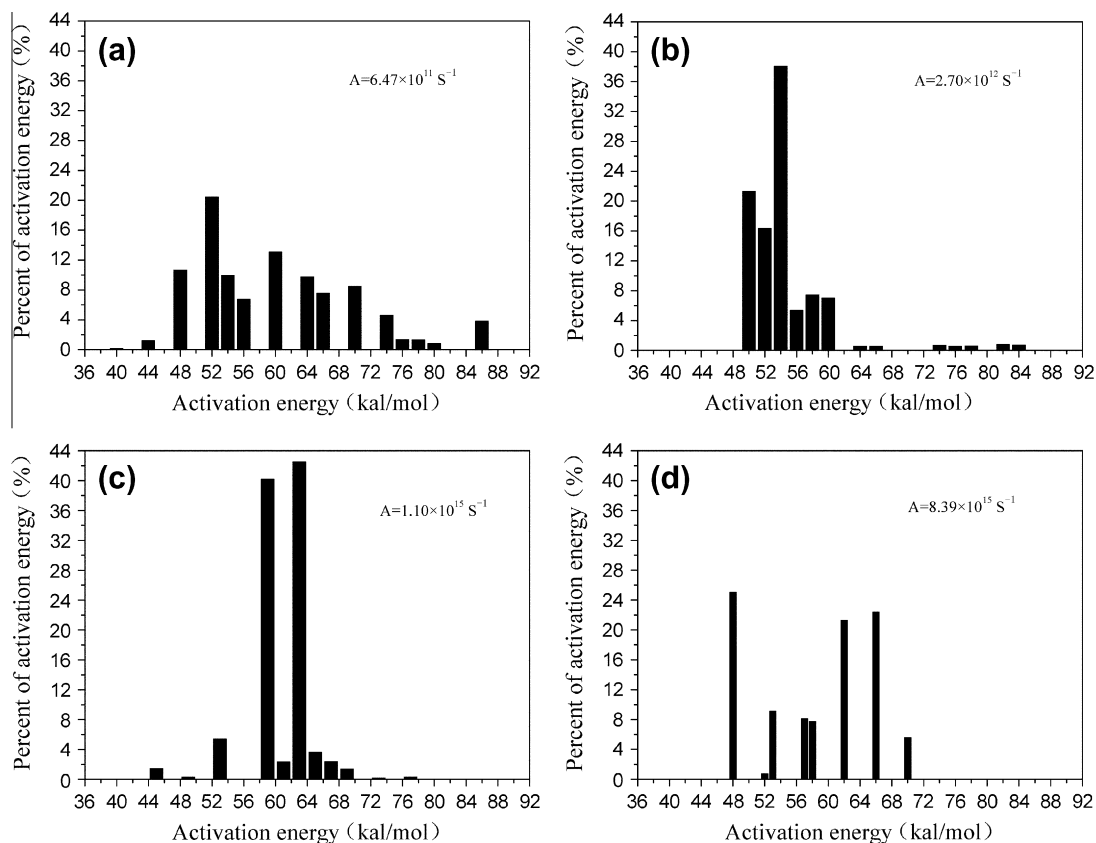


Fig. 3. Kinetic parameters of hydrocarbon gas generation: (a) Methane; (b) Ethane; (c) Propane; (d) Heavy hydrocarbons.

rately linked necessarily to the ULMGG for the source rock determined during the natural gas maturation process.

#### 4.2.1. Expression of the main gas generation period

The predecessors usually expressed the formation of oil and gas by using geological time (Ma), Ro (%), temperature ( $^{\circ}\text{C}$ ) and burial depth (m). Organic matter will be cracked to hydrocarbon in the geological history with a certain burial depth, and ground temperature increasing rapidly (Zheng et al., 2003), and the thermal evolution speeding up simultaneously. It is chemical reactions in the process of type II kerogen cracking macromolecules, and further cleavage of small molecules. Gas generation yield is different in a various thermal stage, which is the process of amount of thermogenic gas of methane-based generated after oil generation. A large number of natural gas will generate in a certain stage, which most of gas products yield is generated. And it is the main period that the hydrocarbon source rocks generate gas, namely the main gas generation period (Wang et al., 2005). Hydrocarbon gas generated from types II kerogen in the deepwater continental slope of the QDNB, the VR expresses generally both the stage in gas generation and the range of the main gas generation period. But the key problem is how to determine the boundary of Ro in the main gas generation period.

#### 4.2.2. Determination of the main gas generation period

The progressive process of the hydrocarbon gas generation under the closed-system conditions at different temperature can be determined by obtaining the evolution of hydrocarbon gas with the cumulative and phase rate of hydrocarbon gas products (Hu et al., 2004; Zhao et al., 2005). In contrast, the interval process of hydrocarbon gas generation obtained at different temperature under the open-system conditions is conducive to accurately under-

stand the different characters in the stages of the evolution of hydrocarbon gas generation (Liu et al., 2009). Natural gas produced during the main gas generation period can attribute to 60–80% of the total gas production derived from hydrocarbon source rocks (Wang et al., 2005; Zhao et al., 2005).

As the integrated research on the geological conditions in the deepwater continental slope of the QDNB and the analysis of experimental results, the present study to determine the main gas generation period for type II kerogen include that: (i) Natural gas produced during the main gas generation period can attribute to no less than 60% of the total gas production; (ii) what is the inflexion between the slope of the curve of natural gas generation rate and its transformation ratio. As pointed out above for the present study on kinetics of the experimental data from type II kerogen in the deepwater continental slope of the QDNB, it is assumed that the transformation ratio of natural gas generation is the same 20% and 80% of the total gas production corresponding to the onset and end of the main gas generation period as Wang et al. (2005) and Zhao et al. (2005).

### 4.3. The ULMGG of the whole rock from type II kerogen

#### 4.3.1. Determination of the ULMGG by comparison method

Reflectance measurements made on minor to trace amounts of vitrinite dispersed within the predominantly amorphous kerogen gave consistently higher mean reflectance values under anhydrous conditions. To set up the entire thermal evolution of the whole rock as a potential gas source in the QDNB, VR of pyrolysis residues was recorded with range from 0.50% to 5.05% under hydrous closed-system conditions at different temperature for 72 h and at the final temperature level ( $500^{\circ}\text{C}$ ) for different duration (72, 144 and 216 h).

The cumulative rates of methane observe in Fig. 4a increasing gradually with increasing maturation and predominantly higher than that of ethane, propane and heavy hydrocarbons from type II kerogen. Evidently,  $R_o$  related to the peak maximum of the phase rates for the former is equal to 3.0% more than that of the latter, which is 2.53% (Fig. 4b). The cumulative and phase rates of ethane, propane and heavy hydrocarbons decrease gradually over 2.53% $R_o$  and cease completely about 3.0% $R_o$ . Experimental results indicate that methane generated from ethane, propane and heavy hydrocarbons after the VR of 2.53% $R_o$  at 400 °C except for degradation of kerogen under the closed-system conditions. It is the time for natural gas generation that peaks maximum of the hydrocarbon gas generation in the maturity process is the highest transformation ratio of hydrocarbon gas generation. Experimental results indicate that the ULMGG of the whole rock for type II kerogen is more than 3.0% $R_o$ , which is peak maximum of methane yield. The previous studies show that amounts of liquids hydrocarbon (e.g., crude oil) cracking during the main gas generation period was the involvement of thermal cracking of  $C_{2+}$  by the close-system pyrolysis (Hu et al., 2004; Zhao et al., 2005), which is prolonged the peak maximum of hydrocarbon generation to higher stages of the thermal evolution for 3.0% $R_o$  due to the presence of secondary methane. The cumulative rate of methane has increased dramatically at 500 °C for 144 h ( $R_o = 4.38\%$ ) more than for 72 h

( $R_o = 4.06\%$ ), but changed little for 216 h ( $R_o = 5.05\%$ ), where corresponding final pressure recorded are 10.2, 10.4, and 10.4 MPa, respectively. When  $R_o$  is between 0.50% and 4.38%, the increasing range of methane is very large but very low over 4.38% for  $R_o$ . And hydrocarbon gas generation from the hydrocarbon source rock does not nearly occur in the end evolution of  $R_o$  over 4.38%. Therefore, the ULMGG of type II kerogens is equal to 4.38% $R_o$ .

In addition, compared to the experimental results in the closed system pyrolysis, Fig. 4c and d shows the hydrocarbon gas generation curves for methane, ethane, propane and heavy hydrocarbons. Those curves are obtained in the open-system non-isothermal pyrolysis with the heating rate of 20 °C/min. The cumulative rates of hydrocarbon gas generation increased gradually with increasing maturation in the range from 0.50% to 5.79% $R_o$ .  $R_o$  related to the peak maximum of those hydrocarbon gas generation except for propane (1.29%) is equal to 1.62% $R_o$ . It is obvious that the peak maximum is lower in the open system than in the closed system for 3.0% $R_o$ . Experimental results support that the conclusions of the experimental data of hydrocarbon gas generation from degradation of kerogen more earlier than from liquid hydrocarbons cracking, such as crude oil (Hu et al., 2004; Zhao et al., 2005).

Furthermore, Fig. 4d exhibit that the main generation period for ethane, propane and heavy hydrocarbons is very narrow and conspicuous in the range from 450 to 650 °C. It is worthy of discussion

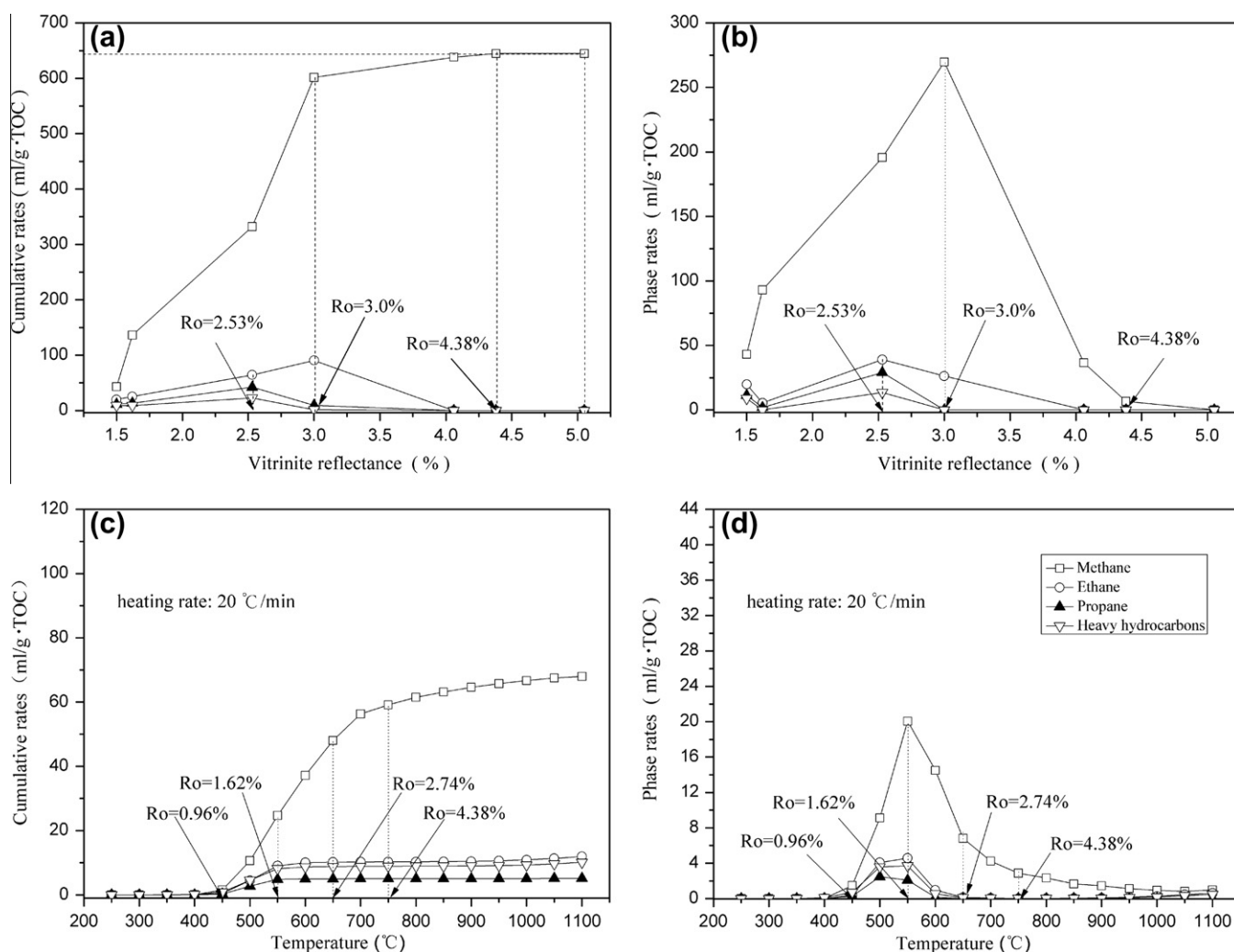


**Fig. 4.** Characteristics of the hydrocarbon gas generation rates in the pyrolysis experiments: (a) the cumulative rates in the closed-system experiment; (b) the phase rates in the closed-system experiment; (c) the cumulative rates in the open-system experiment; (d) the phase rates in the open-system experiment. The high heating rate of the open-system experiment is 20 °C/min related to the present-day high geothermal fields in the Qiongdongnan Basin.

that methane is characterized by a very broad range during the main gas generation period. Because methane only remains in the gas phase due to other hydrocarbon gas cracking to methane at high maturity levels (Tissot and Welte, 1984). The cumulative and phase rate of hydrocarbon gas generation for ethane, propane and heavy hydrocarbons changes little after VR of 4.38% related to 750 °C. So, the experimental results indicate that the ULMGG of the whole rock of type II kerogen related to VR of 4.38% is reasonable.

A  $\Delta Ro$ -value, given a definition of the difference between higher temperature and lower temperature, has been calculated from all values of Ro in the range from 0.44% to 5.79% in open-system non-isothermal experiment at the rate of 20 °C/min related to the present-day high geothermal fields in the QDNB (Fig. 5, Table 3). VR of all segments had an increasing trend. And the increasing rate of VR both in segments A–B and C–D is sufficiently lower than in segments B–C.

Although the thermal evolution of organic matter maturity during a pyrolysis can be demonstrated by the evolution curve of the vitrinite reflectance vs. temperature plot as shown in Fig. 5, it showed merely an increasing trend and could not properly express the details. The  $\Delta Ro$ -value proposed in this paper has advantages over value of VR for the thermal evolution of organic matter maturity. And it is more useful for the details described as well as the cumulative and/or phase rates of hydrocarbon gas generation vs. temperature curve in Fig. 4c and d, especially in the maximum increase of the segments B–C of VR.

Furthermore, its evolution exhibited different features in different stages (Fig. 5 and Table 3). In the first stage, the  $\Delta Ro$  in segments E–F had a slight increasing trend, because the corresponding VR in segments A–B was the lower increasing rate. In the second stage, the steepening of the  $\Delta Ro$  of segments F–G was sufficiently fast such that the  $\Delta Ro$  increased rapidly from 0.02% to 0.30% during the onset of the main generation period for natural gas ranging from 0.96% to 2.74%Ro. In the third stage, the  $\Delta Ro$  of segments G–H had a slow increasing trend during the middle portion of the main generation period for natural gas. The evolution of the  $\Delta Ro$  in the fourth stage of segments H–I was similar to the second stage, but the values were much higher, from 0.30% up to 0.80%, during the end of the main generation period for natural gas. The  $\Delta Ro$  of the fifth stage for segments I–K was the same as the third stage, but the values were over 0.80% with a distinct peak maximum of 0.83% at J point, evidently, where the value corresponding to Ro is equal to 4.38%. Moreover, a clear decrease of the  $\Delta Ro$  evolution for Ro over 4.38% is observed in the sixth stage of segments K–L from 0.80% to about 0.10%. And the  $\Delta Ro$  evolution

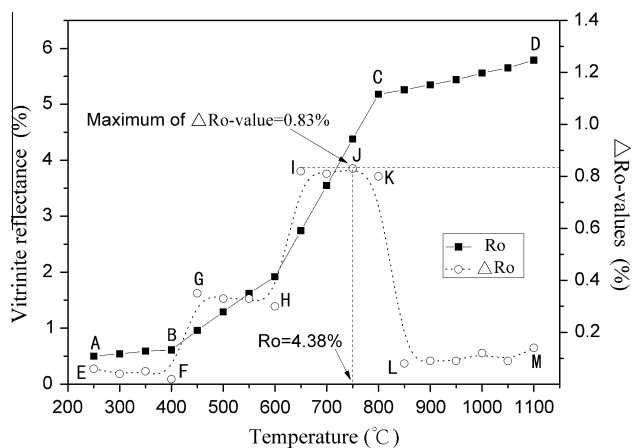


Fig. 5. Vitrinite reflectance and its corresponding  $\Delta Ro$ -values vs. temperature in the open-system non-isothermal experiment. The high heating rate of the open-system non-isothermal experiment is 20 °C/min.

Table 3

The data on  $\Delta Ro$  (%) related to Ro (%), and temperature (°C) in the open-system non-isothermal experiment at the heating rate of 20 °C/min.

No.	T (°C)	Ro (%)	$\Delta Ro$ (%)
Unheated		0.44	
1	250	0.5	0.06
2	300	0.54	0.04
3	350	0.59	0.05
4	400	0.61	0.02
5	450	0.96	0.35
6	500	1.29	0.33
7	550	1.62	0.33
8	600	1.92	0.30
9	650	2.74	0.82
10	700	3.55	0.81
11	750	4.38	0.83
12	800	5.18	0.80
13	850	5.26	0.08
14	900	5.35	0.09
15	950	5.44	0.09
16	1000	5.56	0.12
17	1050	5.65	0.09
18	1100	5.79	0.14

had a slight increasing trend in the value around 0.1% of the final stage of segments L–M. It is the same value of the ULMGG equal to 4.38%Ro and corresponding to the maximum of  $\Delta Ro$ -value for 0.83% as the aforementioned conclusion.

#### 4.3.2. Determination of the ULMGG by kinetics method

As Fu et al. (2002), the curves of the natural gas transformation ratio in the open-system non-isothermal pyrolysis with two constant heating rates are obtained by kinetic method (Fig. 6). The main gas generation period for natural gas determined is ranging from 0.96% to 2.74% by combination the transformation ratio of natural gas generation (20–80%) with the discontinuity in the slope of the curve of natural gas generation rate and its transformation ratio (Fu et al., 2002; Wang et al., 2005; Zhao et al., 2005). It is the same range as the aforementioned conclusion by comparison to the experimental results from the gas generation rates under open system conditions. The natural gas transformation ratio for ethane, propane and heavy hydrocarbons over 90% changes little after 750 °C related to VR of 4.38%.

Methane can be destroyed, VR of more than 4.0%, at the last stage of metamorphism for the source rock, where the constituents of the residual kerogen are converted to graphitic carbon as Tissot and Welte (1984). Other extensive hydrocarbon thermal simulation experiments indicate that the gas generation rate from the mudstone of source rock is slower for VR of about 3.0% (Hu et al., 2004) and gas will not be generated, VR of about 4.0%. The ULMGG from type II kerogen of the experimental results is from 4.4% to 4.5% (Wang et al., 2005). Chen et al. (2007) presented in details the experimental data yielded by Rock-Eval pyrolysis, kerogen atomic H/C, Py-GC and gold-tube sealing thermal simulation on the marine Cambrian–Ordovician source rock (the Tarim Basin) and revealed that the ULMGG or the “deadline of gas generation” for marine types I and II kerogen is equal to 3.0% of VR; while the “deadline of gas generation” for type III kerogen typically like coals is as high as 10%Ro (Fig. 7a). It is no wonder there existed various viewpoints as pointed out above on the upper limit of maturity for different organic matter to generate gases in days gone by. It has been demonstrated that type III organic matter like coal releases hydrogen more slowly than the marine type I or II organic matter during the thermal evolution, suggesting a lower hydrocarbon generative rate but a longer thermal evolutionary phase of hydrocarbon generation. And different organic matter has obviously different utmost maturities for gas generation. It is therefore slight different conclusion between the previous and the present



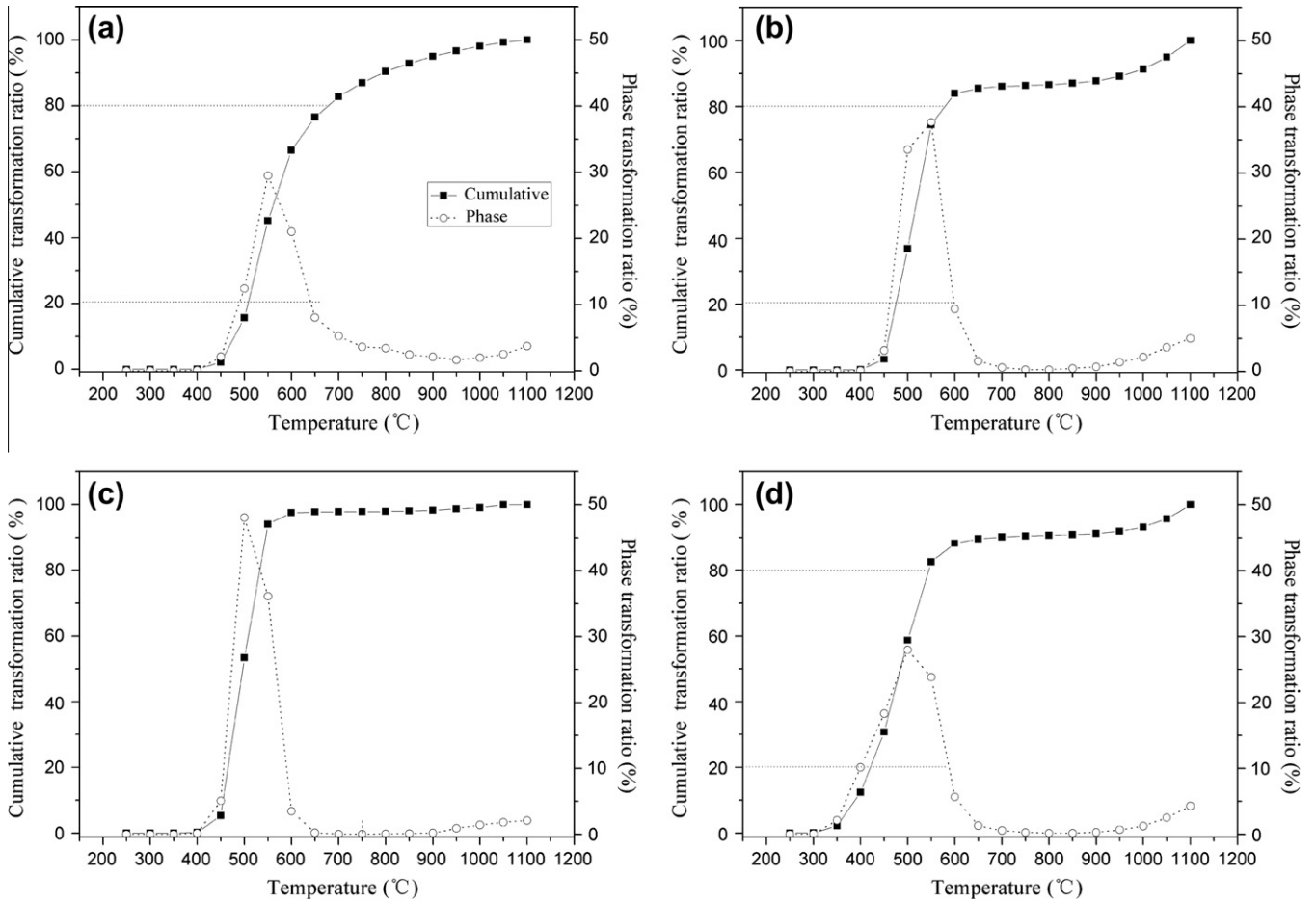


Fig. 6. The cumulative and phase translation ratio of hydrocarbon gas generation in the open-system non-isothermal experiment: (a) Methane; (b) Ethane; (c) Propane; (d) Heavy hydrocarbons.

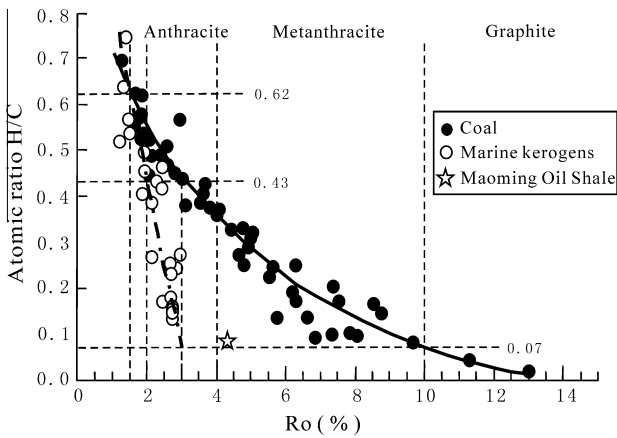


Fig. 7. Variations in H/C atomic ratios of coal and marine kerogens with increasing maturity (revised after Chen et al., 2007).

(Tissot and Welte, 1984; Hu et al., 2004; Wang et al., 2005; Chen et al., 2007).

4.4. The potential of Yacheng formation in the deepwater continental slope basin

Basic geological conditions for the migration and accumulation model of the deepwater continental slope in the QDNB are similar

to those of the shallow-water continental shelf, nevertheless, the deeper the sag and fractures, the bigger the dimensions of the deposits and infillings, and hence the dimensions of the source rock of Yacheng formation in the deepwater continental slope basin are larger and can lay an abundant source foundation for oil and gas generation in the deepwater continental slope. The hydrocarbon source rock of Yacheng formation revealed by drilled well in the shallow-water continental shelf include carbonaceous mudstone with coaly organic matter, and dark mudstone. Coal is ubiquitous in the source rock of Yacheng formation, and the cumulative thickness of coal is about 6 m and the predominant consists of coal is clarain (Zhu et al., 2007). According to Chen et al. (2007), the ULMGG for marine types I or II kerogen is equal to 3.0%Ro; while the ULMGG for type III kerogen typically like coal is as high as 10%Ro. And the ULMGG of the source rock of Yacheng formation for type II kerogen is equal to VR of 4.38% as the present experimental results.

In addition, Ro on a series of selected 8 wells (Fig. 8) is ranging from 0.46% to 2.19% and average for 1.02% related to the burial depth of the source rock of Yacheng formation between 3700 and 5500 m. According to the classic theory by Tissot and Welte (1984), the hydrocarbon source rock of Yacheng formation is in the stage of condensate and wet gas formation by further pyrolysis of dry gas and still effective for generating hydrocarbons. Most of the hydrocarbon source rock of Yacheng formation is still far from reaching the ULMGG for type II kerogen according to the present and previous results (Tissot and Welte, 1984; Hu et al., 2004; Wang et al., 2005; Chen et al., 2007). The hydrocarbon source rock of

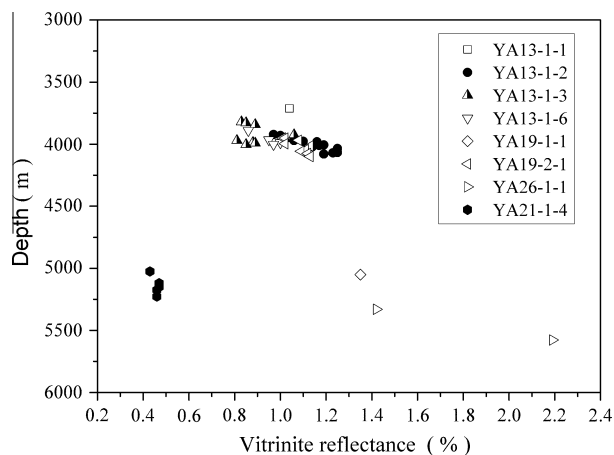


Fig. 8. Vitritine reflectance from the drilled wells for the source rock of Yacheng formation in the shallow-water continental shelf of the Qiongdongnan Basin.

Yacheng formation in the deepwater continental slope basin have still preferable natural gas generative potential, where  $R_o$  is more than 0.7% (Shan, 2010), especially in the local along the central depression belt from the depocenter to both the margin and adjacent areas in the QDNB of the SCS.

## 5. Conclusions

As reaction kinetic parameters of the hydrocarbon gas generation from experimental results, the quantitative model of immature organic material of the whole rock for type II kerogen at the different stage of the evaluation in the deepwater continental slope of the QDNB are obtained. The activation energies and corresponding pre-exponential factors for methane, ethane, propane, and heavy hydrocarbons ( $C_{4-6}$ ) were in the range from 38 to 86 kcal/mol at  $6.47 \times 10^{11}$  (1/s), 44 to 92 kcal/mol at  $2.70 \times 10^{12}$  (1/s), 43 to 77 kcal/mol at  $1.10 \times 10^{15}$  (1/s) and 46 to 70 kcal/mol at  $8.39 \times 10^{15}$  (1/s), respectively.

The characteristics of the evolution of hydrocarbon gas generation were analyzed systematically by both comparing to the rates and study on kinetics of the hydrocarbon gas generation from the open-system non-isothermal pyrolysis at two constant heating rates conditions with ultra-high temperature. It indicates that hydrocarbon gas generation during the main gas generation period is ranging from 0.96% to 2.74% $R_o$ .  $\Delta R_o$ -values increased rapidly from 0.02% up to 0.30% and from 0.30% up to 0.80% related to the onset and the end of the main gas generation period. The upper limit of maturity for gas generation of the whole rock for type II kerogen is equal to 4.38% $R_o$  with a slight difference as the previous results, where the gas generation rates change little with the increase of maturation, the  $\Delta R_o$ -value is 0.83% of the maximum related to VR of 4.38% $R_o$  and the hydrocarbon source rock don't nearly occur in the end process of natural gas generation while  $R_o$  is over 4.38%. It shows that it is the same the ULMGG from the whole rock for type II kerogen as the method with both comparison and kinetics.

According to the present conclusions, we replied positively the key questions that the hydrocarbon source rock of Yacheng formation in the deepwater continental slope basin has still preferable natural gas generative potential, particularly in the local along the central depression belt from the depocenter to both the margin and adjacent areas in the QDNB. It help to evaluate the resource potential for oil and gas of the hydrocarbon source rock in the deepwater continental slope with lower exploration in the northern of the South China Sea. And it is very significant to petroleum

exploration and development in the deepwater continental slope basin of the broad ocean areas in China.

## Acknowledgements

This work was financially supported jointly by the National Natural Science Foundation of China (Grant No.: 40972099) the Important Direction Project of Knowledge Innovation in Resource and Environment Field, Chinese Academy of Sciences (Grant No.: KZCX2-EW-QN112) and the National Petroleum Major Projects (Grant Nos.: 2011ZX05005 and 2011ZX05008).

## References

- Béhar, F., Vandenbroucke, M., Tang, M., Marquis, F., Espitalié, J., 1997. Thermal cracking of kerogen in open and closed systems: determination of kinetic parameters and stoichiometric coefficients for oil and gas generation. *Organic Geochemistry* 26, 321–339.
- Braun, R.L., Burnham, A.K., 1987. Analysis of chemical reactions kinetics using a distribution of activation energies and simpler models. *Energy Fuels* 1, 153–161.
- Braun, R.L., Burnham, A.K., 1992. PMOD: a flexible model of oil and gas generation and expulsion. *Organic Geochemistry* 19, 161–172.
- Carr, A.D., 1999. A vitritine reflectance kinetic model incorporating overpressure retardation. *Marine and Petroleum Geology* 16, 355–377.
- Carr, A.D., 2000. Suppression and retardation of vitritine reflectance, Part 2. Derivation and testing of a kinetic model for suppression. *Journal of Petroleum Geology* 23, 475–496.
- Carr, A.D., Williamson, J.E., 1990. The relationship between aromaticity, vitritine reflectance and maceral composition of coals: implications for the use of vitritine reflectance as a maturation parameter. *Organic Geochemistry* 16, 313–323.
- Chen, J.P., Zhao, W.Z., Xiao, Z.Y., Zhang, S.C., Deng, C.P., Sun, Y.G., Wang, Z.M., 2007. A discussion on the upper limit of maturity for gas generation by marine kerogens and the utmost of gas generative potential: taking the study on the Tarim Basin as an example. *Chinese Science Bulletin* 52, 95–100.
- Dalla Torre, M., Mahlmann, R.F., Ernst, W.G., 1997. Experimental study on the pressure dependence of vitritine maturation. *Geochimica et Cosmochimica Acta* 61, 2921–2928.
- Espitalié, J., Ungerer, P., Irwin, I., Marquis, F., 1988. Primary cracking of kerogens. Experimenting and modelling  $C_1$ ,  $C_{2-5}$ ,  $C_{6-15}$  and  $C_{15+}$  classes of hydrocarbons formed. *Organic Geochemistry* 13, 893–899.
- Forbes, P.L., Ungerer, P.M., Kuhfuss, A.B., Riis, F., Eggen, S., 1991. Compositional modelling of petroleum generation and expulsion: trial application to a local mass balance in the Smørbukk Field, Haltenbanken area, Norway. *American Association of Petroleum Geologists Bulletin* 75, 873–893.
- Fu, J.M., Xu, F.F., Chen, D.Y., Liu, D.H., Hu, C.Y., Jia, R.F., Xu, S.P., Brassell, A.S., Eglinton, G., 1985. Biomarker compounds of biological inputs in Maoming oil shale. *Geochimica* 02, 99–114 (in Chinese).
- Fu, S.Y., Peng, P.A., Zhang, W.Z., Liu, J.Z., Zan, C.L., 2002. Kinetic study of the hydrocarbon generation from upper Paleozoic coals in Ordos Basin. *Science in China (Series D)* 32, 812–818 (in Chinese).
- Geng, X.H., Geng, A.S., Xiong, Y.Q., Liu, J.Z., Zhang, H.Z., Zhao, Q.F., 2005. Kinetic simulating experiment on marine carbonate source comparison of source rocks with isolated kerogens. *Geochimica* 34, 612–618 (in Chinese).
- Goff, J.C., 1983. Hydrocarbon generation and migration from Jurassic source rocks in the East Shetland Basin and Viking Graben of the Northern North Sea. *Journal of the Geological Society* 140, 445–474.
- Gong, Z.S., Li, S.T., Xie, T.J., Zhang, Q.M., Xu, S.C., 1997. Continental Margin Basin Analysis and Hydrocarbon Accumulation in Northern South China Sea. Science Press, pp. 1–126 (in Chinese).
- Guo, M., Zhou, M.W., Li, R., Yu, D.Y., 2009. Analysis on oil shale forming conditions in Maoming Basin of Guangdong Province. *Geology and Mineral Resources of South China* 2, 47–55 (in Chinese).
- Hao, F., Sun, Y.C., Li, S.T., Zhang, Q.M., 1995. Overpressure retardation of organic matter maturation and petroleum generation: a case study from the Yinggehai and Qiongdongnan Basins, South China Sea. *American Association of Petroleum Geologists Bulletin* 79, 551–562.
- He, L.J., Wang, K.L., Xiong, L.P., Wang, J.Y., 2001. Heat flow and thermal history of the South China Sea. *Physics of the Earth and Planetary Interiors* 126, 211–220.
- He, J.X., Chen, S.H., Cui, S.S., Ma, W.H., Luan, X.W., 2009. Early-stage prediction and evaluation of hydrocarbon source rock in the deep basin on the northern continental margin of the South China Sea. *Geology in China* 36, 404–416 (in Chinese).
- Hou, D.J., Wang, P.R., Lin, R.Z., Li, S.J., 1989. Light hydrocarbons in pyrolysis gas of Maoming Oil Shale and its thermal evolution significance. *Journal of Jiangnan Petroleum Institute* 11, 7–11 (in Chinese).
- Hu, G.Y., Li, Z.S., Luo, X., Li, J., Jiang, Z.S., Wang, C.Y., 2004. The comparison of gas generation potential and model between two different thermal simulation systems. *Acta Sedimentologica Sinica* 14, 134–139 (in Chinese).

- Huang, W.L., 1996. Experimental study of vitrinite maturation: effects of temperature, time, pressure, water, and hydrogen index. *Organic Geochemistry* 24, 233–241.
- Huang, B.J., 1999. Gas potential and its favorable exploration areas in Qiongdongnan Basin. *Natural Gas Industry* 19, 34–39 (in Chinese).
- Hunt, J.M., 1979. *Petroleum Geochemistry and Geology*. W. H. Freeman, San Francisco, p. 617.
- Khorasani, G.K., Michelsen, J.K., 1994. The effects of overpressure, lithology, chemistry and heating rate on vitrinite reflectance evolution, and its relationship with oil generation. *Australian Petroleum Exploration Association Journal* 34, 418–435.
- Krooss, B.M., Leythaeuser, D., Lillack, H., 1993. Nitrogen-rich natural gases—Qualitative and quantitative aspects of natural gas accumulation in reservoirs. *Erdöl Und Kohle Erdgas, Petroleum Organic Geochemistry* 46, 271–276.
- Krooss, B.M., Littke, R., Müller, B., Frielingsdorf, J., Schwochau, K., Idiz, E.F., 1995. Generation of nitrogen and methane from sedimentary organic matter: implications on the dynamics of natural gas accumulations. *Chemical Geology* 126, 291–318.
- Lewan, M.D., 1998. Experiments on the role of water in petroleum formation. *Geochimica et Cosmochimica Acta* 61, 3691–3723.
- Li, X.X., Zhu, G.H., 2005. The fault system and its hydrocarbon carrier significance in Qiongdongnan Basin. *China Offshore Oil and Gas* 17, 1–7 (in Chinese).
- Li, X.Q., Xiao, X.M., Mi, J.K., Tang, Y.C., Xiao, Z.Y., Liu, D.H., Shen, J.G., Yang, Y.F., Wang, Y., Dong, P., 2008. Kinetic parameters of methane generated from source rocks in the Kuqa Depression of Tarim Basin and their application. *Acta Geologica Sinica* 82, 154–163.
- Liu, Q.Y., Krooss, B.M., Jin, Z.J., Wang, Y., Hollenstein, J., Littke, R., Liu, W.H., 2009. Determination of kinetic parameters in open system non-isothermal pyrolysis with ultra-high temperature for coal and its macerals and geological extrapolation of natural gas. *Earth Science Frontiers* 16, 167–172 (in Chinese).
- Mi, L.J., Yuan, Y.S., Zhang, G.C., Hu, S.B., He, L.J., Yang, S.C., 2009. Characteristics and genesis of geothermal field in deep-water area of the northern South China Sea. *Acta Petrolei Sinica* 30, 27–32 (in Chinese).
- Pepper, A.S., Corvi, P.J., 1995. Simple kinetic models of petroleum formation. Part 1: Oil and gas generation from kerogen. *Marine and Petroleum Geology* 12, 291–319.
- Price, L.C., Wenger, L.M., 1992. The influence of pressure on petroleum generation and maturation as suggested by aqueous pyrolysis. *Organic Geochemistry* 19, 141–159.
- Qin, J.Z., Liu, J.W., Liu, B.Q., Guo, J.Y., Jin, J.C., Wang, D.L., Guo, S.Z., Yu, G.Y., 2002. Hydrocarbon yield and geochemical parameters affected by heating time and added water amount in the simulation test. *Petroleum Geology & Experiment* 24, 152–157 (in Chinese).
- Ritter, U., 1984. The influence of time and temperature on vitrinite reflectance. *Organic Geochemistry* 6, 473–480.
- Schaefer, R.G., Schenk, H.J., Hardelauf, H., Harmsa, R., 1990. Determination of gross kinetic parameters for petroleum formation from Jurassic source rocks of different maturity levels by means of laboratory experiments. *Organic Geochemistry* 16, 115–120.
- Shan, J.N., 2010. The thermal evolution of the hydrocarbon source rocks in the deepwater area of the Qiongdongnan Basin. In: *The Academic Conference of Oil and Gas Accumulation and Exploration in the Deepwater Basin of South China Sea*. Haikou, Hainan, pp. P111–P117.
- Shi, X.B., Qiu, X.L., Xia, K.Y., Zhou, D., 2003. Characteristics of surface heat flow in the South China Sea. *Journal of Asian Earth Sciences* 22, 265–277.
- Sun, J.L., 1994. The characteristics of YA13-1 gas field of the South China Sea and its enrichment pool-formed conditions. *Natural Gas Industry* 14, 1–7 (in Chinese).
- Sweeney, J.J., Burnham, A.K., 1990. Evaluation of a simple model of vitrinite reflectance based on chemical kinetics. *American Association of Petroleum Geologists Bulletin* 74, 1559–1570.
- Tissot, B.P., Welte, D.H., 1984. *Petroleum Formation and Occurrence*. Springer Verlag, Berlin Heidelberg, New York, pp. 1–699.
- Wang, Y.P., Zhao, C.Y., Wang, Z.Y., Wang, H.J., Zou, Y.R., Liu, J.Z., Zhao, W.Z., Geng, A.S., Liu, D.H., Lu, J.L., 2005. Kinetic method for determining the main gas generation period of marine organic matters and its application. *Petroleum Exploration and Development* 32, 153–155 (in Chinese).
- Waples, D.W., 1980. Time and temperature in petroleum formation: application of Lopatin's method to petroleum exploration. *American Association of Petroleum Geologists Bulletin* 64, 916–926.
- Yu, P., Wang, J.L., Zhong, H.Z., Chen, B., Liu, T.S., Liu, X.K., 1999. Comprehensive geophysical research on the basement structure in Qiongdongnan Basin. *China Offshore Oil and Gas (Geology)* 13, 443–450 (in Chinese).
- Yu, Z.Q., Peng, P.A., Sheng, G.Y., Fu, J.M., 2000. Study on carbon isotope of biomarker from Tertiary oil shale in both Maoming and Jiangnan basin. *Chinese Science Bulletin* 45, 2783–2789 (in Chinese).
- Yuan, Y.S., Yuan, C., Hu, S.B., He, L.J., 2008. Tectonic subsidence of Qiongdongnan Basin and its main control factors. *Chinese Journal of Geophysics* 51, 248–255 (in Chinese).
- Yuan, Y.S., Zhu, W.L., Mi, L.J., Hu, S.B., He, L.J., 2009. "Uniform geothermal gradient" and heat flow in the Qiongdongnan and Pearl River Mouth Basins of the South China Sea. *Marine and Petroleum Geology* 26, 1152–1162.
- Zhan, W.H., Zhu, Z.Y., Sun, L.T., Sun, Z.X., Yao, Y.T., Qiu, X.L., 2006. The epoch and diversities of Neotectonic Movement in the South China Sea. *Acta Geologica Sinica* 80, 491–496 (in Chinese).
- Zhang, G.C., Mi, L.J., Wu, S.G., Tao, W.X., He, S.B., Lü, J.J., 2007. Deepwater area—the new prospecting targets of northern continental margin of South China Sea. *Acta Petrolei Sinica* 28, 15–21 (in Chinese).
- Zhang, G.C., Zhu, W.L., Mi, L.J., Zhang, H.H., Liang, J.S., Qu, H.J., 2010. The theory of hydrocarbon generation controlled by source rock and heat from circle distribution of outside-oil fields and inside-gas fields in South China Sea. *Acta Sedimentologica Sinica* 28, 987–1005 (in Chinese).
- Zhao, W.Z., Wang, Z.Y., Zhang, S.C., Wang, H.J., Zhao, C.Y., Hu, G.Y., 2005. Successive generation of natural gas from organic materials and its significance in future exploration. *Petroleum Exploration and Development* 32, 1–7 (in Chinese).
- Zheng, J.J., Wen, D.S., Men, Q.X., Ji, L.M., Sun, G.Q., 2003. Characteristics of geochemical parameters of coal measures source rock in the thermal simulation experiment. *Natural Gas Geoscience* 14, 134–139 (in Chinese).
- Zhu, W.L., Zhang, G.C., Yang, S.K., Li, X.S., Shi, H.S., Pang, X., Luo, Z.Q., Huang, B.J., He, M., 2007. *Geology of Natural Gas in Northern Continental Marginal Basin of South China Sea*. Petroleum Industry Press, pp. 1–391 (in Chinese).
- Zhu, W.L., Zhang, G.C., Gao, L., 2008. Geological characteristics and exploration objectives of hydrocarbons in the northern continental margin basin of South China Sea. *Acta Petrolei Sinica* 29, 1–9 (in Chinese).
- Zou, Y.R., Peng, P.A., 2001. Overpressure retardation of organic matter maturation: a kinetics model and its application. *Marine and Petroleum Geology* 18, 707–713.